

## Phospha(III)guanidinate complexes of titanium(IV) and zirconium(IV) amides

Natalie E. Mansfield, Joanna Grundy, Martyn P. Coles\*, Peter B. Hitchcock

Department of Chemistry, University of Sussex, Falmer, Brighton, BN1 9QJ, UK

### ARTICLE INFO

#### Article history:

Received 6 April 2010

Accepted 19 May 2010

Available online 1 June 2010

#### Keywords:

Coordination compounds

Titanium amides

Zirconium amides

Phosphaguanidinate

Crystal structure

### ABSTRACT

Two procedures for the synthesis of group 4 phosphaguanidine compounds  $M(R_2PC\{NR'\}_2)(NR''_2)_3$  ( $M = Ti, Zr$ ;  $R = Ph, Cy$ ;  $R' = ^iPr, Cy$ ;  $R'' = Me, Et$ ) are described. Spectroscopic characterization indicated symmetrical bonding of the phosphaguanidinate ligand in solution for the *P*-diphenyl derivatives whereas the *P*-dicyclohexyl analogs adopt a more rigid geometry with inequivalent  $N_{amide}$  substituents within the phosphaguanidinate ligand. X-ray diffraction studies show exclusively monomeric *tbp* metal centers for a series of derivatives, with a chelating phosphaguanidinate ligand that spans an axial and an equatorial position. Two different conformers have been identified in the solid-state that differ in the relative orientation of the phosphorus  $R_2P-C$  substituents with respect to the equatorial plane of the *tbp* metal. The synthetic protocol was extended to the bimetallic complex,  $[PhP\{C(N^iPr)_2Ti\{NMe_2\}_3\}CH_2-]_2$ , which was characterized by crystallography as the *meso*-form.

© 2010 Elsevier Ltd. All rights reserved.

### 1. Introduction

The phosphaguanidinate anion,  $[R_2PC\{NR'\}_2]^-$ , is a versatile ligand that continues to elicit attention since it was first investigated by Thewissen et al. in 1980 [1]. In the original studies, the rhodium and iridium phosphine complexes **A** were reported (Fig. 1), for which spectroscopic data indicated a square planar metal with a chelating  $\kappa^1-P,N$ -bonding mode. The first structurally characterized example,  $ZrCp'_2[(Me_3Si)_2PC\{NPh\}_2]Cl$  (**B**), was synthesized by carbodiimide insertion into a terminal phosphide to afford the chelating  $\kappa^1-N,N'$ -phosphaguanidinate [2,3], reminiscent of traditional amidinate and guanidinate bonding [4–9,10].

We became interested in this area as an extension of our work with metal guanidine [11] and guanidinate complexes [10], initially developing a synthetic route to the neutral, *P*-diphenyl substituted ligand precursors  $Ph_2PC\{NR'\}\{NHR'\}$  [12], via lithium phosphaguanidinate **C** and **D** [13]. Synthesis of the bulky derivatives  $R_2PC\{NAr\}\{NHAr\}$  ( $Ar = 2,6\text{-}^iPr_2C_6H_3$ ,  $R = Ph, Cy$ ) has recently been described using a similar synthetic procedure [14]. Building on this work, other groups have demonstrated that tetra-substituted phosphaguanidines may be obtained catalytically from the reaction of carbodiimides with secondary phosphines in the presence of alkali-metal reagents [15,16], group 2 metal amides [17,18], transition metal phosphides [19] or lanthanide compounds [20].

Crystallographic characterization of phosphaguanidinate complexes has demonstrated versatility in the bonding. The *P*-diphenyl substituted lithium salts **C** and **D** exhibit the  $\kappa^1-P,N$ - and  $\kappa^1,2-N-\kappa^1-N'$ -bonding modes, respectively, with the more conventional

$\kappa^1-N,N'$ -bonding mode observed at aluminum [21], and more recently at lanthanum (**E**) [20]. Chelating  $\kappa^1-P,N$ -coordination, originally deduced from spectroscopic data to be present in **A**, is reported in the homoleptic Co(II) compound [22], with related bonding reported in the patent literature for ethylene polymerization pre-catalysts containing bulky phosphaguanidinate ligands [23]. The base-free lithium salt derived from the *P*-dicyclohexyl derivative  $Cy_2PC\{NR'\}\{NHR'\}$  [24], crystallized as a bridging ligand with  $\kappa^1-P,N$ -bonding to one metal and secondary  $N_{imine}$   $\cdot\cdot Li$  bonds, generating cyclic hexamer (**F**) [22]. Finally Jones and co-workers have observed a novel chelating mode for phosphaguanidinate  $[Cy_2PC\{NAr\}_2]^-$  ( $Ar = 2,6\text{-}^iPr_2C_6H_3$ ) at Ti(I) and In(I) centers [25,26]. The metal is coordinated in an  $\eta^1$ -fashion by the amido nitrogen, with an approximately  $\eta^3$ -interaction with the aryl substituent of the other nitrogen (**G**).

One of the driving forces behind our research was to develop multi-metallic complexes through simultaneous amidinate and phosphine coordination. This was recently demonstrated with the structurally characterized mixed aluminum/copper compound,  $CuBr(Ph_2PC\{N^iPr\}_2AlMe_2)_2$  (**H**) [27], indicating that only minor perturbations occur to the bonding within the ligand when combining with two metal fragments (Fig. 2). We have also developed alkyl-bridged *bis*-phosphaguanidines [28]. The bimetallic aluminum complex,  $[PhP\{C(N^iPr)_2AlMe_2\}CH_2-]_2$  (**I**) was isolated as a mixture of the *rac*- and *meso*-products that could be separated by fractional crystallization.

Gathering further information on the types of complex that these versatile ligands adopt remains a worthwhile pursuit and, as such, we wish to report in this contribution the synthesis and structural characterization of a series of titanium and zirconium amides supported by examples of the phosphaguanidinate ligand.

\* Corresponding author. Tel.: +44 0 1273 877339; fax: +44 0 1273 677196.  
E-mail address: [m.p.coles@sussex.ac.uk](mailto:m.p.coles@sussex.ac.uk) (M.P. Coles).

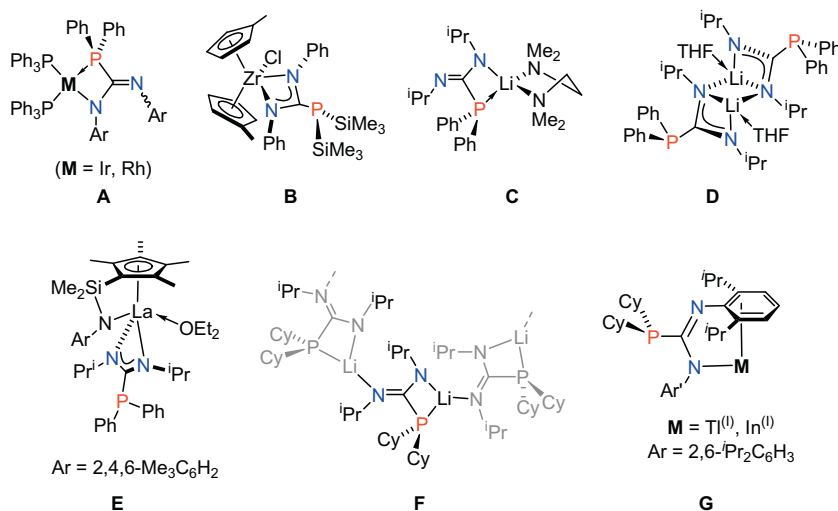


Fig. 1. Examples of different bonding modes in phosphaguanidinate metal complexes.

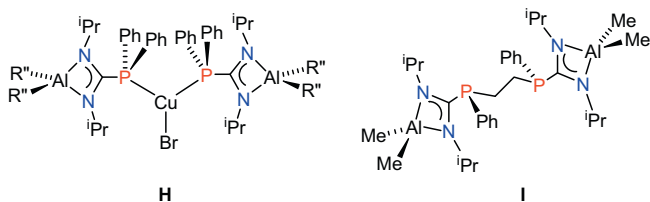


Fig. 2. Examples of bimetallic and linked phosphaguanidinate complexes.

## 2. Experimental

### 2.1. General considerations

All manipulations were carried out under dry nitrogen using standard Schlenk-line and cannula techniques, or in a conventional nitrogen-filled glovebox. Solvents were dried over appropriate drying agents and degassed prior to use. NMR spectra were recorded using a Bruker Avance DPX 300 MHz spectrometer at 300.1 ( $^1\text{H}$ ), 75.4 ( $^{13}\text{C}\{^1\text{H}\}$ ) and 121.4 ( $^{31}\text{P}\{^1\text{H}\}$ ) MHz and a Bruker AMX 500 MHz spectrometer at 500.1 ( $^1\text{H}$ ), 125.7 ( $^{13}\text{C}\{^1\text{H}\}$ ) and 202.4 ( $^{31}\text{P}\{^1\text{H}\}$ ) MHz, from samples at 25 °C in [ $^2\text{H}_6$ ]-benzene, unless otherwise stated. Coupling constants are quoted in Hz. Proton and carbon chemical shifts were referenced internally to residual solvent resonances; phosphorus chemical shifts were referenced externally to  $\text{H}_3\text{PO}_4$  (aq). Elemental analyses were performed by S. Boyer at London Metropolitan University.

$\text{Zr}(\text{NMe}_2)_4$  [29],  $\text{Ph}_2\text{PC}\{\text{NR}'\}\{\text{NHR}'\}$  (**1**) [12],  $\text{Cy}_2\text{PC}\{\text{NR}'\}\{\text{NHR}'\}$  (**2**) [24],  $[\text{PhP}\{\text{C}\{\text{N}^i\text{Pr}\}\{\text{NH}^i\text{Pr}\}\text{CH}_2\text{-}]_2$  (**7**) [28] were made according to literature procedures. The corresponding lithium phosphaguanidinate species  $[\text{Li}(\text{R}_2\text{PC}\{\text{NR}'\}_2)(\text{solvent})_n]_k$  were prepared in situ by reacting **1** and **2** with  $^n\text{BuLi}$  [13,22].  $\text{TiCl}_4$ ,  $\text{ZrCl}_4$ ,  $\text{Ti}(\text{NEt}_2)_4$  and  $\text{Ti}(\text{NMe}_2)_4$  were purchased from Sigma–Aldrich; 0.20 M stock solutions of the tetraamide were made by diluting the neat compound with the appropriate amount of hexane. A 1.0 M solution of  $[\text{Ti}(\text{NMe}_2)_3\text{Cl}]$  and  $[\text{Zr}(\text{NMe}_2)_3\text{Cl}]$  in toluene/hexane were made by combining the appropriate molar quantities of the metal tetraamide and tetrachloride [30]. Compounds listed in inverted commas indicate that they were not isolated and used in situ; for the purposes of calculating yields and reaction stoichiometries, the yield was assumed to be quantitative.

### 2.2. General synthesis – procedure 1

$^n\text{BuLi}$  (1 equiv.) was added dropwise via syringe to a stirred solution of the neutral phosphaguanidine in THF at 0 °C. After stirring at ambient temperature for 1 h the volatiles were removed under reduced pressure and the resultant white solid was washed with hexane ( $2 \times 10$  mL). The residual solid was dissolved in toluene added dropwise to a solution of  $[\text{M}(\text{NMe}_2)_3\text{Cl}]$  in toluene at  $-78$  °C. The reaction mixture was allowed to warm to ambient temperature affording a clear solution and a white precipitate. Removal of the volatiles and extraction with hexane, followed by concentration and storage at  $-30$  °C yielded the product as a crystalline solid.

### 2.3. General synthesis – procedure 2

A clear solution of the appropriate metal-amide in hexanes was added dropwise via syringe to a clear colorless solution of the neutral phosphaguanidine in toluene at ambient temperature. The resulting solution was stirred for  $\sim 15$  h. Removal of the volatile component, followed by storage of a concentrated hexane solution at  $-30$  °C yielded the product as a crystalline solid.

#### 2.3.1. $\text{Ti}(\text{Ph}_2\text{PC}\{\text{N}^i\text{Pr}\}_2)(\text{NMe}_2)_3$ (**3a**)

Compound **3a** was made according to procedure 2, using the following amounts:  $\text{Ti}(\text{NMe}_2)_4$  (1.60 mL of a 0.20 M solution in hexanes, 0.32 mmol) and  $\text{Ph}_2\text{PC}\{\text{N}^i\text{Pr}\}\{\text{NH}^i\text{Pr}\}$  (0.10 g, 0.32 mmol). The compound was isolated as yellow crystals. Yield 0.08 g (52%).  $^1\text{H}$  NMR (300 MHz):  $\delta$  7.65 (t,  $J = 7.1$ , 4H,  $m\text{-C}_6\text{H}_5$ ), 7.13–7.03 (m, 6H,  $o\text{-}$  and  $p\text{-C}_6\text{H}_5$ ), 4.20 (sept,  $J = 6.2$ , 2H,  $\text{CHMe}_2$ ), 3.31 (s, 18H,  $\text{NMe}_2$ ), 0.92 (d,  $J = 6.2$ , 12H,  $\text{CHMe}_2$ ).  $^{13}\text{C}$  NMR (75 MHz):  $\delta$  173.2 (d,  $J = 56$ ,  $\text{PCN}_2$ ), 134.7 (d,  $J = 16$ ,  $\text{C}_6\text{H}_5$ ), 132.5 (d,  $J = 18$ ,  $\text{C}_6\text{H}_5$ ), 128.9 (d,  $J = 6$ ,  $\text{C}_6\text{H}_5$ ), 128.5 ( $\text{C}_6\text{H}_5$ ), 50.7 (d,  $J = 17$ ,  $\text{CHMe}_2$ ), 46.4 ( $\text{NMe}_2$ ), 24.9 ( $\text{CHMe}_2$ ).  $^{31}\text{P}$  NMR (121 MHz):  $\delta$   $-23.0$ .

#### 2.3.2. $\text{Ti}(\text{Ph}_2\text{PC}\{\text{NCy}\}_2)(\text{NMe}_2)_3$ (**3b**)

Compound **3b** was made according to procedure 1, using the following amounts:  $^n\text{BuLi}$  (0.44 mL of a 2.5 M solution in hexanes, 1.1 mmol),  $\text{Ph}_2\text{PC}\{\text{NCy}\}\{\text{NHCy}\}$  (0.39 g, 1.0 mmol),  $[\text{Ti}(\text{NMe}_2)_3\text{Cl}]$  (1.00 mL of a 1.0 M solution in toluene/hexane, 1.0 mmol). The compound was isolated as dark yellow crystals. Yield 0.07 g (50%).

Compound **3b** was also made according to procedure 2, using the following amounts:  $\text{Ti}(\text{NMe}_2)_4$  (1.25 mL of a 0.20 M solution in hexanes, 0.25 mmol) and  $\text{Ph}_2\text{PC}\{\text{NCy}\}\{\text{NHCy}\}$  (0.10 g,

0.25 mmol). The compound was isolated as yellow crystals. Yield 0.07 g (50%).  $^1\text{H}$  NMR (300 MHz):  $\delta$  7.66 (t,  $J = 8.4$ , 4H,  $m\text{-C}_6\text{H}_5$ ), 7.13–7.02 (m, 6H,  $o$ - and  $p\text{-C}_6\text{H}_5$ ), 3.76 (m, 2H,  $\text{Cy-H}_\alpha$ ), 3.34 (s, 18H,  $\text{NMe}_2$ ), 1.59–0.99 (m, 20H,  $\text{Cy-CH}_2$ ).  $^{13}\text{C}$  NMR (75 MHz):  $\delta$  173.3 (d,  $J = 56$ ,  $\text{PCN}_2$ ), 135.0 (d,  $J = 16$ ,  $\text{C}_6\text{H}_5$ ), 132.5 (d,  $J = 18$ ,  $\text{C}_6\text{H}_5$ ), 128.9 (d,  $J = 6$ ,  $\text{C}_6\text{H}_5$ ), 128.3 ( $\text{C}_6\text{H}_5$ ), 58.9 (d,  $J = 17$ ,  $\text{Cy-C}_\alpha$ ), 46.5 ( $\text{NMe}_2$ ), 35.5 ( $\text{N-Cy}$ ), 26.2 ( $\text{N-Cy}$ ), 26.1 ( $\text{N-Cy}$ ).  $^{31}\text{P}$  NMR (121 MHz):  $\delta$  –22.1.

### 2.3.3. $\text{Ti}(\text{Ph}_2\text{PC}\{\text{N}^i\text{Pr}\}_2)(\text{NEt}_2)_3$ (**3a'**)

Heating an equimolar mixture of  $\text{Ph}_2\text{PC}\{\text{N}^i\text{Pr}\}\{\text{NH}^i\text{Pr}\}$  and  $\text{Ti}(\text{NEt}_2)_4$  to 120 °C in toluene afforded a small number of yellow crystals that were analyzed by elemental analysis and X-ray crystallography. Insufficient pure material was isolated for spectroscopic analysis.

### 2.3.4. $\text{Zr}(\text{Ph}_2\text{PC}\{\text{N}^i\text{Pr}\}_2)(\text{NMe}_2)_3$ (**4a**)

Compound **4a** was made according to procedure 2, using the following amounts:  $\text{Zr}(\text{NMe}_2)_4$  (0.09 g, 0.31 mmol) and  $\text{Ph}_2\text{PC}\{\text{N}^i\text{Pr}\}\{\text{NH}^i\text{Pr}\}$  (0.10 g, 0.31 mmol). The compound was isolated as colorless crystals. Yield 0.11 g (58%).  $^1\text{H}$  NMR (300 MHz):  $\delta$  7.62 (t,  $J = 7.7$ , 4H,  $m\text{-C}_6\text{H}_5$ ), 7.11–7.02 (m, 6H,  $o$ - and  $p\text{-C}_6\text{H}_5$ ), 4.20 (sept,  $J = 6.1$ , 2H,  $\text{CHMe}_2$ ), 3.12 (s, 18H,  $\text{NMe}_2$ ), 0.93 (d,  $J = 6.1$ , 12H,  $\text{CHMe}_2$ ).  $^{13}\text{C}$  NMR (125.5 MHz):  $\delta$  134.4 (d,  $J = 16$ ,  $\text{C}_6\text{H}_5$ ), 132.3 (d,  $J = 18$ ,  $\text{C}_6\text{H}_5$ ), 128.9 (d,  $J = 6$ ,  $\text{C}_6\text{H}_5$ ), 128.6 ( $\text{C}_6\text{H}_5$ ), 50.5 (d,  $J = 18$ ,  $\text{CHMe}_2$ ), 42.6 ( $\text{NMe}_2$ ), 24.8 ( $\text{CHMe}_2$ ).  $\text{PCN}_2$  resonance not observed due to low solubility.  $^{31}\text{P}$  NMR (121 MHz):  $\delta$  –20.8.

### 2.3.5. $\text{Zr}(\text{Ph}_2\text{PC}\{\text{NCy}\}_2)(\text{NMe}_2)_3$ (**4b**)

Compound **4a** was made according to procedure 2, using the following amounts:  $\text{Zr}(\text{NMe}_2)_4$  (0.07 g, 0.25 mmol) and  $\text{Ph}_2\text{PC}\{\text{NCy}\}\{\text{NHCy}\}$  (0.10 g, 0.25 mmol). The compound was isolated as colorless crystals. Yield 0.12 g (67%).  $^1\text{H}$  NMR (300 MHz):  $\delta$  7.64 (t,  $J = 7.2$ , 4H,  $m\text{-C}_6\text{H}_5$ ), 7.11–7.01 (m, 6H,  $o$ - and  $p\text{-C}_6\text{H}_5$ ), 3.77 (m, 2H,  $\text{Cy-H}_\alpha$ ), 3.15 (s, 18H,  $\text{NMe}_2$ ), 1.57–0.93 (m, 20H,  $\text{Cy-CH}_2$ ).  $^{13}\text{C}$  NMR (125 MHz):  $\delta$  175.2 (d,  $J = 55$ ,  $\text{PCN}_2$ ), 134.7 (d,  $J = 16$ ,  $\text{C}_6\text{H}_5$ ), 132.4 (d,  $J = 19$ ,  $\text{C}_6\text{H}_5$ ), 128.9 (d,  $J = 6$ ,  $\text{C}_6\text{H}_5$ ), 128.6 ( $\text{C}_6\text{H}_5$ ), 58.1 (d,  $J = 17$ ,  $\text{Cy-C}_\alpha$ ), 42.7 ( $\text{NMe}_2$ ), 35.6, 26.1, 26.0 ( $\text{Cy-CH}_2$ ).  $^{31}\text{P}$  NMR (121 MHz):  $\delta$  –20.6.

### 2.3.6. $\text{Ti}(\text{Cy}_2\text{PC}\{\text{N}^i\text{Pr}\}_2)(\text{NMe}_2)_3$ (**5a**)

Compound **5a** was made on an NMR scale in  $\text{C}_6\text{D}_6$  according to procedure 2, using the following amounts:  $\text{Ti}(\text{NMe}_2)_4$  (0.007 g, 0.032 mmol) and  $\text{Cy}_2\text{PC}\{\text{N}^i\text{Pr}\}\{\text{NH}^i\text{Pr}\}$  (0.010 g, 0.032 mmol). A conversion of ~90% was noted from the integration of the  $^1\text{H}$  NMR spectrum.  $^1\text{H}$  NMR (300 MHz):  $\delta$  4.67 (m, 1H,  $\text{CHMe}_2$ ), 4.40 (m, 1H,  $\text{CHMe}_2$ ), 3.10 (s, 18H,  $\text{NMe}_2$ ), 1.70–1.24 (m, 22H,  $\text{Cy}$ ), 1.18 (d,  $J = 6.3$ , 12H,  $\text{CHMe}_2$ ).  $^{13}\text{C}$  NMR (75 MHz):  $\delta$  178.0 (d,  $J = 57$ ,  $\text{PCN}_2$ ), 50.2 ( $\text{CHMe}_2$ ), 42.3 ( $\text{NMe}_2$ ), 35.7 (d,  $J = 17$ ,  $\text{Cy-C}_\alpha$ ), 33.3 (d,  $J = 23$ ,  $\text{Cy-CH}_2$ ), 31.6 (d,  $J = 12$ ,  $\text{Cy-CH}_2$ ), 27.2, 27.1, 26.9, 26.6 ( $\text{Cy-CH}_2$ ), 25.2 ( $\text{CHMe}_2$ ).  $^{31}\text{P}$  NMR (121 MHz):  $\delta$  –9.8.

### 2.3.7. $\text{Ti}(\text{Cy}_2\text{PC}\{\text{NCy}\}_2)(\text{NMe}_2)_3$ (**5b**)

Compound **5b** was made according to procedure 2, using the following amounts:  $\text{Ti}(\text{NMe}_2)_4$  (1.25 mL of a 0.2 M solution in hexanes, 0.25 mmol) and  $\text{Cy}_2\text{PC}\{\text{NCy}\}\{\text{NHCy}\}$  (0.10 g, 0.25 mmol). The compound was isolated as yellow crystals. Yield 0.07 g (48%).  $^1\text{H}$  NMR (300 MHz):  $\delta$  4.48 (m, 1H,  $\text{NCy-H}_\alpha$ ), 4.26 (m, 1H,  $\text{NCy-H}_\alpha$ ), 3.32 (s, 18H,  $\text{NMe}_2$ ), 2.18–1.14 (m, 42H,  $\text{P-}$  and  $\text{NCy-CH}_2$ ).  $^{13}\text{C}$  NMR (75 MHz):  $\delta$  178.1 (d,  $J = 57$ ,  $\text{PCN}_2$ ), 59.3 (br,  $\text{NCH}$ ), 46.4 ( $\text{NMe}_2$ ), 36.2 (d,  $J = 17$ ,  $\text{PCy-C}_\alpha$ ), 35.8 (br,  $\text{NCy-CH}_2$ ), 33.2 (d,  $J = 22$ ,  $\text{PCy-CH}_2$ ), 32.0 (d,  $J = 13$ ,  $\text{PCy-CH}_2$ ), 27.4, 27.3, 27.1, 26.6, 26.5, 26.2, 26.1 ( $\text{P-}$  and  $\text{NCy-CH}_2$ ). The  $\text{NCy-CH}_2$  resonances are not clear due to overlap with the  $\text{PCy-CH}_2$  signals and broadening of the signals.  $^{31}\text{P}$  NMR (121 MHz):  $\delta$  –11.0.

### 2.3.8. $\text{Zr}(\text{Cy}_2\text{PC}\{\text{N}^i\text{Pr}\}_2)(\text{NMe}_2)_3$ (**6a**)

Compound **6a** was made according to procedure 2, using the following amounts:  $\text{Zr}(\text{NMe}_2)_4$  (0.09 g, 0.32 mmol) and  $\text{Cy}_2\text{PC}\{\text{N}^i\text{Pr}\}\{\text{NH}^i\text{Pr}\}$  (0.10 g, 0.32 mmol). The compound was isolated as colorless crystals. Yield 0.10 g (58%).  $^1\text{H}$  NMR (300 MHz):  $\delta$  4.82 (m, 1H,  $\text{CHMe}_2$ ), 3.91 (m, 1H,  $\text{CHMe}_2$ ), 3.12 (s, 18H,  $\text{NMe}_2$ ), 1.68–1.26 (m, 22H,  $\text{Cy-CH}_2$ ), 1.19 (br d,  $J = 5.9$ , 12H,  $\text{CHMe}_2$ ).  $^{13}\text{C}$  NMR (125 MHz):  $\delta$  50.3 (d,  $J = 16$ ,  $\text{CHMe}_2$ ), 42.5 ( $\text{NMe}_2$ ), 35.5 (d,  $J = 17$ ,  $\text{Cy-C}_\alpha$ ), 31.6 (d,  $J = 14$ ,  $\text{Cy-CH}_2$ ), 27.1, 27.0, 26.9, 26.4 ( $\text{Cy-CH}_2$ ), 25.1 ( $\text{CHMe}_2$ ).  $\text{PCN}_2$  and  $\text{CHMe}_2$  resonances not observed due to broadening and low solubility.  $^{31}\text{P}$  NMR (121 MHz):  $\delta$  –7.4.

### 2.3.9. $\text{Zr}(\text{Cy}_2\text{PC}\{\text{NCy}\}_2)(\text{NMe}_2)_3$ (**6b**)

Compound **6b** was made according to procedure 2, using the following amounts:  $\text{Zr}(\text{NMe}_2)_4$  (0.07 g, 0.32 mmol) and  $\text{Cy}_2\text{PC}\{\text{NCy}\}\{\text{NHCy}\}$  (0.10 g, 0.32 mmol). The compound was isolated as colorless crystals. Yield 0.13 g (67%).  $^1\text{H}$  NMR (300 MHz):  $\delta$  4.32 (br m, 1H,  $\text{NCy-H}_\alpha$ ), 3.48 (br m, 1H,  $\text{NCy-H}_\alpha$ ), 3.14 (s, 18H,  $\text{NMe}_2$ ), 1.80–1.16 (m, 42H,  $\text{Cy}$ ).  $^{13}\text{C}$  NMR (75 MHz):  $\delta$  178.9 (d,  $J = 54$ ,  $\text{PCN}_2$ ), 58.4, 58.2 (br,  $\text{NCy-C}_\alpha$ ), 42.7 (s,  $\text{NMe}_2$ ), 36.1 (d,  $J = 17$ ,  $\text{PCy-C}_\alpha$ ), 36.0 ( $\text{N-Cy}$ ), 33.2 (d,  $J = 23$ ,  $\text{PCy-CH}_2$ ), 31.8 (d,  $J = 12$ ,  $\text{PCy-CH}_2$ ), 27.4, 27.2, 27.1, 26.4, 26.2 ( $\text{P-}$  and  $\text{NCy-CH}_2$ ). The  $\text{NCy-CH}_2$  resonances are not clear due to overlap with the  $\text{PCy-CH}_2$  signals and broadening of the signals.  $^{31}\text{P}$  NMR (121 MHz):  $\delta$  –8.7.

### 2.3.10. $[\text{PhP}\{\text{C}(\text{N}^i\text{Pr})_2\text{Ti}\{\text{NMe}_2\}_3\}\text{CH}_2\text{-}]_2$ (**8a**)

Compound **8a** was made according to procedure 2, using the following amounts:  $\text{Ti}(\text{NMe}_2)_4$  (2.00 mL of a 0.2 M solution in hexanes, 0.40 mmol) and  $[\text{PhP}\{\text{C}(\text{N}^i\text{Pr})\}\{\text{NH}^i\text{Pr}\}\text{CH}_2\text{-}]_2$  (0.10 g, 0.20 mmol). The compound was isolated as yellow crystals. Yield 0.08 g (47%).  $^1\text{H}$  NMR (300 MHz,  $\text{CDCl}_3$ ):  $\delta$  7.59–7.37 (m, 20H,  $\text{C}_6\text{H}_5$  major and minor isomers), 4.16 (m, 2H,  $\text{CHMe}_2$  major), 3.31 (s, 18H,  $\text{NMe}_2$  minor), 3.30 (s, 18H,  $\text{NMe}_2$  major), 2.20 (d,  $J = 6.4$ , 4H,  $\text{C}_2\text{H}_4$  major) 2.76 (m, 2H,  $\text{CHMe}_2$  minor), 1.30 (d,  $J = 6.0$ , 4H,  $\text{C}_2\text{H}_4$  minor), 1.20 (d,  $J = 6.3$ , 12H,  $\text{CHMe}_2$  minor), 0.89 (d,  $J = 6.3$ , 12H,  $\text{CHMe}_2$  major).  $^{31}\text{P}$  NMR (121 MHz):  $\delta$  –30.6 (*meso*), –31.8 (*rac*). Due to the sparing solubility of this compound in hydrocarbon and decomposition in chlorinated solvents, over extended time periods, it was not possible to obtain accurate  $^{13}\text{C}$  NMR data.

## 2.4. Details of crystallographic study

Details of the crystal data, intensity collection and refinement for complexes **3a'**, **3b** and **4b** are collected in Table 1 and for **5a**, **6a**, **6b** and **8a** in Table 2. Crystals were covered in an inert oil and suitable single crystals were selected under a microscope and mounted on a Kappa CCD diffractometer. Data was collected at 173(2) K using Mo  $\text{K}\alpha$  radiation at 0.71073 Å. The structures were refined with SHELXL-97 [31]. In all cases, the H-atom on the amine nitrogen was refined with other H-atoms in riding mode. Additional features of note are described below:

### 2.4.1. $\text{Zr}(\text{Cy}_2\text{PC}\{\text{NCy}\}_2)(\text{NMe}_2)_3$ (**6b**)

There are two independent molecules of the Zr complex and one poorly defined hexane solvate disordered about an inversion center present in the unit cell. The hexane was included with a common isotropic displacement parameter for carbon and with DFIX and FLAT geometry restraints.

### 2.4.2. $[\text{PhP}\{\text{C}(\text{N}^i\text{Pr})_2\text{Ti}\{\text{NMe}_2\}_3\}\text{CH}_2\text{-}]_2$ (**8a**)

The molecule is located on an inversion center.

**Table 1**Crystal structure and refinement data for Ti(Ph<sub>2</sub>PC{N<sup>i</sup>Pr}<sub>2</sub>)(NEt<sub>2</sub>)<sub>3</sub> (**3a'**), Ti(Ph<sub>2</sub>PC{NCy}<sub>2</sub>)(NMe<sub>2</sub>)<sub>3</sub> (**3b**) and Zr(Ph<sub>2</sub>PC{NCy}<sub>2</sub>)(NMe<sub>2</sub>)<sub>3</sub> (**4b**).

	<b>3a'</b>	<b>3b</b>	<b>4b</b>
Formula	C <sub>31</sub> H <sub>54</sub> N <sub>5</sub> PTi	C <sub>31</sub> H <sub>50</sub> N <sub>5</sub> PTi	C <sub>31</sub> H <sub>50</sub> N <sub>5</sub> PZr
Formula weight	575.66	571.63	614.95
Crystal size (mm)	0.40 × 0.35 × 0.15	0.15 × 0.15 × 0.02	0.40 × 0.40 × 0.05
Crystal system	triclinic	triclinic	triclinic
Space group	<i>P</i> $\bar{1}$ (no.2)	<i>P</i> $\bar{1}$ (no.2)	<i>P</i> $\bar{1}$ (no.2)
<i>a</i> (Å)	9.1768(2)	8.4743(2)	8.5324(2)
<i>b</i> (Å)	11.0815(2)	11.8215(2)	11.9182(2)
<i>c</i> (Å)	17.3647(3)	18.1375(4)	18.1919(3)
$\alpha$ (°)	104.301(1)	72.333(2)	72.164(1)
$\beta$ (°)	92.406(1)	76.752(2)	76.872(1)
$\gamma$ (°)	100.157(1)	69.214(2)	69.529(1)
<i>V</i> (Å <sup>3</sup> )	1677.54(6)	1603.50(7)	1634.90(5)
<i>Z</i>	2	2	2
<i>D</i> <sub>calc</sub> (Mg m <sup>-3</sup> )	1.14	1.18	1.25
Absorption coefficient (mm <sup>-1</sup> )	0.33	0.34	0.41
$\theta$ Range for data collection (°)	3.71–25.02	3.75–25.00	3.73–25.05
Reflections collected	17 624	16 771	17 517
Independent reflections ( <i>R</i> <sub>int</sub> )	5826 (0.040)	5533 (0.066)	5679 (0.039)
Reflections with [ <i>I</i> > 2 $\sigma$ ( <i>I</i> )]	5097	4130	5188
Data/restraints/parameters	5826/0/343	5533/0/349	5679/0/349
Goodness-of-fit (GOF) on <i>F</i> <sup>2</sup>	0.992	1.057	1.023
Final <i>R</i> indices [ <i>I</i> > 2 $\sigma$ ( <i>I</i> )]	<i>R</i> <sub>1</sub> = 0.040; <i>wR</i> <sub>2</sub> = 0.102	<i>R</i> <sub>1</sub> = 0.052; <i>wR</i> <sub>2</sub> = 0.098	<i>R</i> <sub>1</sub> = 0.027; <i>wR</i> <sub>2</sub> = 0.063
<i>R</i> indices (all data)	<i>R</i> <sub>1</sub> = 0.048; <i>wR</i> <sub>2</sub> = 0.108	<i>R</i> <sub>1</sub> = 0.084; <i>wR</i> <sub>2</sub> = 0.110	<i>R</i> <sub>1</sub> = 0.032; <i>wR</i> <sub>2</sub> = 0.065
Largest difference in peak and hole (e Å <sup>-3</sup> )	0.52 and -0.33	0.34 and -0.37	0.26 and -0.41

**Table 2**Crystal structure and refinement data for Ti(Cy<sub>2</sub>PC{N<sup>i</sup>Pr}<sub>2</sub>)(NMe<sub>2</sub>)<sub>3</sub> (**5a**), Zr(Cy<sub>2</sub>PC{N<sup>i</sup>Pr}<sub>2</sub>)(NMe<sub>2</sub>)<sub>3</sub> (**6a**), Zr(Cy<sub>2</sub>PC{NCy}<sub>2</sub>)(NMe<sub>2</sub>)<sub>3</sub> (**6b**) and [PhP(C{N<sup>i</sup>Pr}<sub>2</sub>Ti(NMe<sub>2</sub>)<sub>3</sub>)CH<sub>2</sub>]<sub>2</sub> (**8a**).

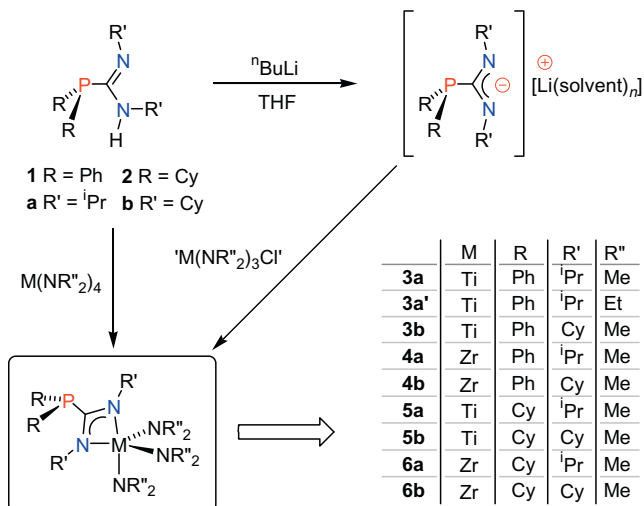
	<b>5a</b>	<b>6a</b>	<b>6b</b>	<b>8a</b>
Formula	C <sub>25</sub> H <sub>54</sub> N <sub>5</sub> PTi	C <sub>25</sub> H <sub>54</sub> N <sub>5</sub> PZr	C <sub>31</sub> H <sub>62</sub> N <sub>5</sub> PZr·0.25(C <sub>6</sub> H <sub>14</sub> )	C <sub>40</sub> H <sub>78</sub> N <sub>10</sub> P <sub>2</sub> Ti <sub>2</sub>
Formula weight	503.60	546.92	648.59	856.86
Crystal size (mm)	0.10 × 0.10 × 0.10	0.10 × 0.05 × 0.02	0.30 × 0.25 × 0.20	0.25 × 0.20 × 0.20
Crystal system	monoclinic	monoclinic	triclinic	triclinic
Space group	<i>P</i> 2 <sub>1</sub> / <i>n</i> (no. 14)	<i>P</i> 2 <sub>1</sub> / <i>n</i> (no. 14)	<i>P</i> $\bar{1}$ (no. 2)	<i>P</i> $\bar{1}$ (no. 2)
<i>a</i> (Å)	8.3493(2)	8.4070(1)	10.4685(1)	8.5743(3)
<i>b</i> (Å)	11.9892(3)	11.9812(2)	10.9017(2)	10.4422(2)
<i>c</i> (Å)	29.5480(6)	29.9250(4)	33.5824(5)	13.7172(4)
$\alpha$ (°)	90	90	97.719(1)	90.085(2)
$\beta$ (°)	91.342(1)	91.462(1)	90.236(1)	98.748(1)
$\gamma$ (°)	90	90	104.032(1)	98.265(2)
<i>V</i> (Å <sup>3</sup> )	2956.99(12)	3013.24(7)	3681.83(9)	1200.93(6)
<i>Z</i>	4	4	4	1
<i>D</i> <sub>calc</sub> (Mg m <sup>-3</sup> )	1.13	1.21	1.17	1.19
Absorption coefficient (mm <sup>-1</sup> )	0.36	0.44	0.37	0.44
$\theta$ Range for data collection (°)	3.40–26.02	3.40–26.04	3.44–26.03	3.41–26.06
Reflections collected	21 559	29 821	43 811	18 286
Independent reflections ( <i>R</i> <sub>int</sub> )	5779 (0.050)	5929 (0.048)	14 375 (0.054)	4735 (0.043)
Reflections with [ <i>I</i> > 2 $\sigma$ ( <i>I</i> )]	4439	4857	10 895	4027
Data/restraints/parameters	5779/0/295	5929/0/295	14 375/11/717	4735/0/250
Goodness-of-fit (GOF) on <i>F</i> <sup>2</sup>	1.017	0.680	1.071	1.053
Final <i>R</i> indices [ <i>I</i> > 2 $\sigma$ ( <i>I</i> )]	<i>R</i> <sub>1</sub> = 0.042; <i>wR</i> <sub>2</sub> = 0.093	<i>R</i> <sub>1</sub> = 0.036; <i>wR</i> <sub>2</sub> = 0.096	<i>R</i> <sub>1</sub> = 0.050; <i>wR</i> <sub>2</sub> = 0.102	<i>R</i> <sub>1</sub> = 0.034; <i>wR</i> <sub>2</sub> = 0.078
<i>R</i> indices (all data)	<i>R</i> <sub>1</sub> = 0.064; <i>wR</i> <sub>2</sub> = 0.102	<i>R</i> <sub>1</sub> = 0.051; <i>wR</i> <sub>2</sub> = 0.112	<i>R</i> <sub>1</sub> = 0.076; <i>wR</i> <sub>2</sub> = 0.113	<i>R</i> <sub>1</sub> = 0.044; <i>wR</i> <sub>2</sub> = 0.082
Largest difference in peak and hole (e Å <sup>-3</sup> )	0.40 and -0.31	0.32 and -0.42	1.00 and -0.52 (near solvate)	0.31 and -0.30

### 3. Results and discussion

Attempted preparation of group 4 metal chlorides M(R<sub>2</sub>PC{NR'<sub>2</sub>}Cl<sub>3</sub>) by the transmetallation reaction between in situ generated lithium phosphaguanidinate and MCl<sub>4</sub> or MCl<sub>4</sub>(THF)<sub>2</sub> (M = Ti, Zr) met with limited success. Whilst an analogous procedure has been successful for a range of 'conventional' guanidinate complexes of group 4 metals [32–41,42], reactions involving the *P*-diphenyl derivatives Ph<sub>2</sub>PC{NR'}{NHR'} (**1a**, R' = <sup>i</sup>Pr; **1b**, R' = Cy) led to complicated mixtures of products. <sup>31</sup>P NMR spectroscopy indicated the presence of tetraphenyldi-phosphine in the crude reaction mixture [ $\delta_P$  -14.8 ppm, C<sub>6</sub>D<sub>6</sub>, 162 MHz] consistent with degradation of the phosphaguanidine via rupture of the P–C<sub>amidine</sub> bond.

The corresponding group 4 amides, M(R<sub>2</sub>PC{NR'<sub>2</sub>})(NR'<sub>2</sub>)<sub>3</sub>, were therefore targeted. Reaction of in situ generated lithium phosphaguanidinate with M(NR'<sub>2</sub>)<sub>3</sub>Cl (M = Ti, Zr) successfully afforded the desired complexes, although the yield was typically less than 30% (Scheme 1). The amine elimination route between the neutral phosphaguanidines **1a,b** and **2a,b** and the metal tetrakis(amides) M(NR'<sub>2</sub>)<sub>4</sub>, however, afforded the desired products in considerably higher yields (48–67%). It was noted that reactions with Ti(NEt<sub>3</sub>)<sub>4</sub> required heating to promote amine elimination, in contrast with the corresponding Ti(NMe<sub>2</sub>)<sub>4</sub> reactions which proceeded at room temperature.

Compounds **3–6** were isolated as yellow (Ti) or colorless (Zr) crystalline materials after purification. In each case <sup>31</sup>P NMR spectroscopy showed a single resonance, in the range  $\delta$  -22.1 to -20.0



**Scheme 1.** Synthetic procedures used in the synthesis of group 4 metal phosphaguanidinate complexes described in this work.

for *P*-diphenyl derivatives (**3** and **4**) and  $\delta$  –11.0 to –7.4 for *P*-dicyclohexyl species (**5** and **6**). <sup>1</sup>H NMR data indicated a phosphaguanidinate:amide ratio of 1:3, consistent with formation of M(L)(NR''<sub>2</sub>)<sub>3</sub> (L = phosphaguanidinate). One set of resonances was observed for each the NR'' substituents of the phosphaguanidinate ligands for compounds **3** and **4**, with a single environment for the amide substituents. This is attributed to a fluxional trigonal bipyramidal complex in solution with fast exchange between the axial and equatorial positions.<sup>1</sup> Low temperature NMR (198 K) did not resolve the spectra, indicating a low-energy barrier to this fluxional process. In contrast, data for the *P*-dicyclohexyl derivatives **5** and **6** showed different environments for the N<sub>amidine</sub> substituents, consistent with a more rigid solution-state structure.

The <sup>1</sup>H, <sup>13</sup>C and <sup>31</sup>P NMR spectra were consistent with the proposed structures M(R<sub>2</sub>PC{NR''<sub>2</sub>})<sub>2</sub>(NR''<sub>2</sub>)<sub>3</sub>.<sup>2</sup> However, combustion analysis results were consistently inaccurate for the formulated compounds, despite repeated attempts on recrystallized samples. Whilst we can not completely rule out the presence of NMR silent contaminants (e.g., metal oxides) an alternative explanation for these erroneous results is the formation of non-volatile metal nitride/carbonitride (or possibly phosphide) materials during the combustion. This is not without precedent, given the all nitrogen coordination environment at the metal centers in these compounds. Indeed, in the last couple of years, conventional guanidinate ligands have been successfully utilized for the stabilization of molecular precursors in the (MO)CVD of a number of nitrogen containing materials including tantalum [43–45,46], niobium [47], tungsten [46,48–50] and gadolinium nitride [51], and titanium carbonitride [42], where the source of the nitrogen typically arises from the guanidinate ligand.

Reactions between two equivalents of the neutral *P*-dicyclohexylphosphaguanidine and M(NR''<sub>2</sub>)<sub>4</sub> yielded only the mono-substituted product species, even after prolonged reflux in toluene solution. This is likely due to the steric crowding at the metal center upon mono-substitution, preventing protonolysis of additional metal–amide bonds; a similar restriction has been noted in the at-

<sup>1</sup> Although this spectroscopic data is also consistent with a square-based pyramid in which the phosphaguanidinate forms two of the basal ligands and the three amides fluctuate between basal and apical positions, this is unlikely given the strong preference for five-coordinate early transition-metals to adopt trigonal bipyramidal geometries. This would also contradict the solid-state data for these complexes.

<sup>2</sup> Representative <sup>1</sup>H, <sup>13</sup>C and <sup>31</sup>P NMR spectra are provided in the Supplementary data.

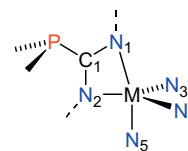


**Fig. 3.** Key for bond length and angle tables.

tempted preparation of bis-guanidinate, Ti[(Me<sub>3</sub>Si)<sub>2</sub>NC{N<sup>i</sup>Pr}<sub>2</sub>]<sub>2</sub>(NMe<sub>2</sub>)<sub>2</sub>, via salt metathesis [42].

X-ray diffraction data have been solved for a number of compounds,<sup>3</sup> and the molecular structures of representative examples are presented in Figs. 4 and 5; crystal structure and refinement data is collected in Tables 1 and 2, and bond lengths and angles in Tables 3 and 4. Fig. 3 presents a generic atomic numbering scheme for the compounds described in this study to facilitate comparison between data for different derivatives.

All compounds contain a five-coordinate metal center in what is best described as a highly distorted trigonal bipyramidal geometry, with  $\tau$ -values [52] in the range 0.55–0.70. As expected for early transition metals, the phosphaguanidinate is present as a  $\kappa^1$ -N,N'-chelating ligand (**B** and **E**, Fig. 1), with axial and equatorial N<sub>amidine</sub> atoms. The acute bite angle of the phosphaguanidinate ligand [ave. 59.3°] is the primary cause of the distortion from t<sub>bp</sub>-geometry, resulting in a significantly reduced N<sub>ax</sub>–M–N<sub>ax</sub> bond angle [range 155.52(11)°–162.78(7)°], as noted in related five-coordinate metal containing structures [42,53–56]. We note a consistently shorter C–N<sub>ax</sub> bond compared to the C–N<sub>eq</sub> (range of  $\Delta_{CN}$  [57]: 0.030–0.046 Å), consistent with partial localization within the amidine unit. This has previously been noted in five-coordinate aluminum compounds supported by amidinate ligands [58], and reflects a greater contribution to the overall bonding from the resonance structure **B** (Fig. 6).

The orientation of the R<sub>2</sub>P-group with respect to the approximate equatorial plane differs within this series of compounds. In the *P*-diphenyl compounds **3b** and **4b** the phosphide group is positioned such that the phenyl substituents point away from the MN<sub>3</sub>-plane ( $\alpha$ -form, Fig. 7), whilst in the *P*-dicyclohexyl substituted examples, the phosphorus groups point towards the equator ( $\beta$ -form). The structure of **3a'**, being the only diethylamido derivative structurally examined, differs from the other *P*-diphenyl examples with respect to its *P*-substituent orientation, crystallizing as the  $\beta$ -form (Fig. 4). In this case, the M–N<sub>axial</sub>–C angles suggest that the increased steric influence of the NEt<sub>2</sub> ligands force the N<sub>axial</sub> substituent back towards the phenyl groups on phosphorus, destabilizing the  $\alpha$ -form (Fig. 7).<sup>4</sup> Whilst it is recognized that these data are from the solid-state structures, and that in solution free rotation about the P–C bond is likely, energetic preferences for a specific orientation of this group will have important consequences in the development of multi-metallic compounds [13,27].

Given the inherent stability of chelating bis-phosphines, and the aforementioned potential application of the compounds described in this manuscript as metal-functionalized phosphines, we were keen to explore the possibility of synthesizing a bimetallic group 4 compound incorporating our previously reported linked bis(phosphaguanidine) [28]. The 1:2 reaction of [PhP(C{N<sup>i</sup>Pr}{NH<sup>i</sup>Pr})CH<sub>2</sub>–]<sub>2</sub> (**7**), with Ti(NMe<sub>2</sub>)<sub>4</sub> was therefore carried out, affording yellow crystals (**8a**) upon crystallization from toluene

<sup>3</sup> The crystal structures of Ti(Ph<sub>2</sub>PC{NCy}<sub>2</sub>)(NMe<sub>2</sub>)<sub>3</sub> (**3b**) and Zr(Cy<sub>2</sub>PC{N<sup>i</sup>Pr}<sub>2</sub>)(NMe<sub>2</sub>)<sub>3</sub> (**6a**) have also been solved. ORTEPs have been included in the Supplementary data.

<sup>4</sup> It is noted that the N<sub>amidine</sub> substituents also differ when comparing **3'a**, **3b** and **4b**. However, previous studies have indicated that these groups have a minimal effect on the metrical parameters associated with the bonding in compounds of this type.

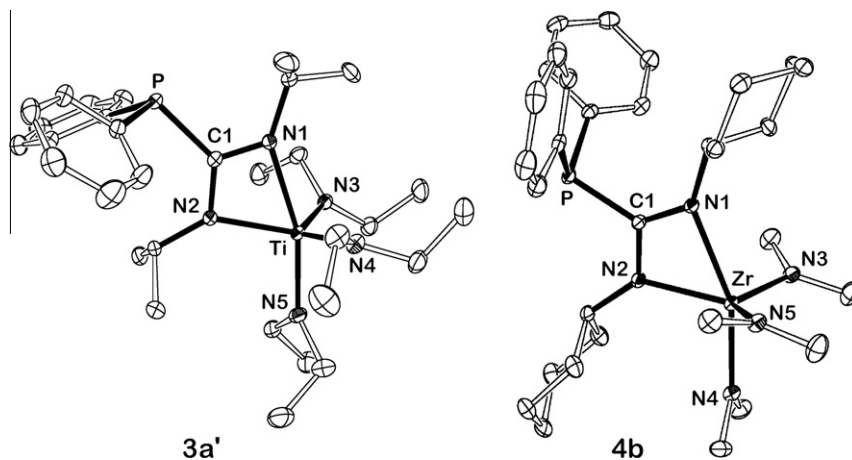


Fig. 4. ORTEP of the molecular structures of Ti(Ph<sub>2</sub>PC(N<sup>i</sup>Pr)<sub>2</sub>)(NEt<sub>2</sub>)<sub>3</sub> (**3a'**) and Zr(Ph<sub>2</sub>PC(NCy)<sub>2</sub>)(NMe<sub>2</sub>)<sub>3</sub> (**4b**). Ellipsoids drawn at 30% probability; hydrogens omitted.

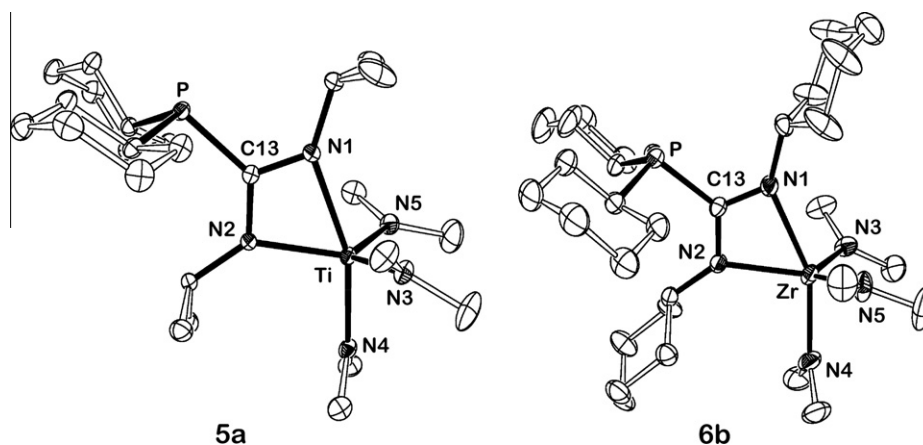


Fig. 5. ORTEP of the molecular structures of Ti(Cy<sub>2</sub>PC(N<sup>i</sup>Pr)<sub>2</sub>)(NMe<sub>2</sub>)<sub>3</sub> (**5a**) and one of the independent molecules of Zr(Cy<sub>2</sub>PC(NCy)<sub>2</sub>)(NMe<sub>2</sub>)<sub>3</sub> (**6b**). Ellipsoids drawn at 30% probability; hydrogens and, in the case of 6b the solvate, omitted.

Table 3

Selected bond lengths (Å) for the compounds M(R<sub>2</sub>PC{NR'<sub>2</sub>})<sub>2</sub>(NR''<sub>2</sub>)<sub>3</sub>. Atomic labeling scheme taken from Fig. 3 to facilitate comparisons of equivalent bonds.

	3a'	3b	4b	5a	6a	6b
N <sub>1</sub> –M	2.251(2)	2.231(2)	2.3396(14)	2.2363(17)	2.333(2)	2.349(3)/2.336(2)
N <sub>2</sub> –M	2.099(2)	2.087(2)	2.2302(15)	2.0878(16)	2.227(2)	2.218(2)/2.220(2)
N <sub>3</sub> –M	1.922(2)	1.895(3)	2.0340(16)	1.9007(18)	2.044(2)	2.043(3)/2.050(3)
N <sub>4</sub> –M	1.908(2)	1.897(2)	2.0304(16)	1.9030(17)	2.037(2)	2.042(3)/2.027(3)
N <sub>5</sub> –M	1.960(2)	1.999(2)	2.0935(16)	1.9682(17)	2.096(2)	2.087(3)/2.085(3)
C <sub>1</sub> –N <sub>1</sub>	1.311(2)	1.311(3)	1.316(2)	1.309(3)	1.320(3)	1.315(4)/1.316(4)
C <sub>1</sub> –N <sub>2</sub>	1.351(2)	1.342(3)	1.346(2)	1.355(3)	1.352(3)	1.356(4)/1.350(4)
C <sub>1</sub> –P	1.888(2)	1.890(3)	1.8914(18)	1.892(2)	1.892(3)	1.895(3)/1.895(3)

Table 4

Selected bond angles (°) for the compounds M(R<sub>2</sub>PC{NR'<sub>2</sub>})<sub>2</sub>(NR''<sub>2</sub>)<sub>3</sub>. Atomic labeling scheme taken from Fig. 3 to facilitate comparisons of equivalent bonds.

	3a'	3b	4b	5a	6a	6b*
N <sub>1</sub> –M–N <sub>5</sub>	162.78(7)	161.24(9)	157.22(6)	160.30(7)	155.64(9)	155.57(11)/157.37(10)
N <sub>1</sub> –M–N <sub>2</sub>	60.91(6)	60.81(9)	57.73(5)	60.84(6)	57.86(8)	57.92(9)/57.82(9)
N <sub>1</sub> –M–N <sub>3</sub>	92.88(7)	94.66(10)	96.44(6)	94.31(7)	94.70(9)	98.43(10)/97.15(10)
N <sub>1</sub> –M–N <sub>4</sub>	93.67(7)	94.94(9)	95.16(6)	96.03(7)	97.74(9)	96.52(12)/95.66(11)
N <sub>5</sub> –M–N <sub>2</sub>	101.93(7)	100.43(9)	99.49(6)	99.60(7)	98.25(9)	97.85(11)/99.56(10)
N <sub>5</sub> –M–N <sub>3</sub>	96.29(7)	94.75(10)	95.49(6)	94.74(8)	94.71(9)	96.46(12)/94.83(11)
N <sub>5</sub> –M–N <sub>4</sub>	95.43(7)	94.81(10)	95.87(6)	95.64(7)	97.97(10)	94.43(14)/96.53(12)
N <sub>2</sub> –M–N <sub>3</sub>	115.44(7)	118.97(10)	118.07(6)	121.85(7)	121.60(9)	118.76(11)/120.69(10)
N <sub>2</sub> –M–N <sub>4</sub>	123.27(7)	118.69(10)	118.46(7)	118.05(7)	117.29(9)	122.29(11)/119.78(10)
N <sub>3</sub> –M–N <sub>4</sub>	115.64(7)	118.34(11)	119.15(7)	116.06(8)	116.76(10)	115.42(12)/115.11(11)

\* Two independent molecules in the unit cell.

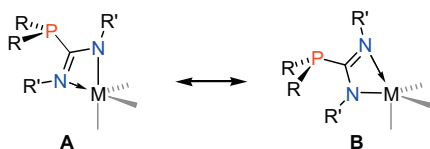


Fig. 6. Resonance structures contributing to the bonding in  $M(R_2PC\{NR'\}_2)(NR''_3)$ .

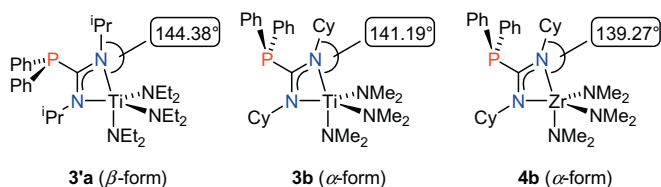
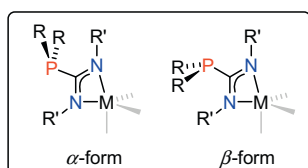
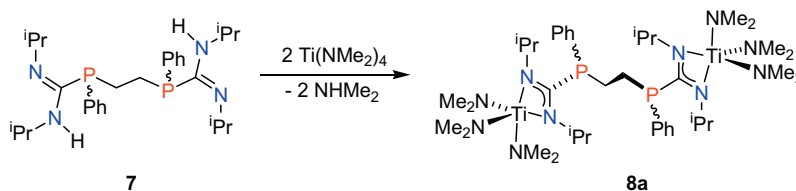


Fig. 7. Conformational differences between  $\alpha$ - and  $\beta$ -forms of the ligand.

(Scheme 2). The  $^{31}\text{P}$  NMR spectrum showed resonances at  $\delta -30.6$  and  $-31.8$ , assigned to the *rac*- and *meso*-forms of the complexes, arising from the chiral phosphine group. The  $^1\text{H}$  NMR spectrum was complicated by the presence of both forms in solution, although groups of peaks corresponding to the expected resonances were observed. Once again, elemental analysis failed to give a result consistent with the expected formulation of **8a**.

The molecular structure of **8a** is illustrated in Fig. 8; crystal structure data is collected in Table 2 and selected bond lengths and angles in Table 5. Compound **8a** crystallizes from toluene as the *meso*-form with both ends of the molecule related by an inversion center. The ligand binds to each titanium as the *N,N'*-chelate forming the expected distorted *tbp*-geometry, with a  $\tau$ -value of 0.68 and the phosphorus substituents in the  $\beta$ -position. With the exception of minor variations, the bonding parameters of **8a** mirror those in the mono-phosphaguanidinate complexes described earlier, suggesting that the metals are sufficiently far apart that they do not have a strong influence on the bonding at the other end of the molecule.

In summary, we have demonstrated a clean route to the mono-phosphaguanidinate complexes,  $M(R_2PC\{NR'\}_2)(NR''_3)$ , via amine elimination. The *P*-diphenyl compounds are fluxional in solution with a rapid exchange of axial and equatorial positions consistent with a low-energy pathway converting these positions in a trigonal bipyramidal geometry, whereas the *P*-dicyclohexyl derivatives are more rigid in solution. No further reactivity with a second equivalent of phosphaguanidine could be induced, suggesting a crowded metal center that restricts the approach of additional neutral ligand precursor.



Scheme 2. Synthesis of the bimetallic compound  $[\text{PhP}\{C(\text{N}^i\text{Pr})_2\text{Ti}(\text{NMe}_2)_3\}\text{CH}_2-]_2$  (**8a**).

Table 5

Selected bond lengths (Å) and angles ( $^\circ$ ) for  $[\text{PhP}\{C(\text{N}^i\text{Pr})_2\text{Ti}(\text{NMe}_2)_3\}\text{CH}_2-]_2$  (**8a**). Atomic labeling scheme taken from Fig. 3 to facilitate comparisons of equivalent bonds.

$\text{N}_1\text{-Ti}$	2.2631(14)	$\text{N}_5\text{-Ti}$	1.9440(15)
$\text{N}_2\text{-Ti}$	2.0689(14)	$\text{C}_1\text{-N}_1$	1.308(2)
$\text{N}_3\text{-Ti}$	1.9130(16)	$\text{C}_1\text{-N}_2$	1.353(2)
$\text{N}_4\text{-Ti}$	1.8941(15)	$\text{C}_1\text{-P}$	1.8917(16)
$\text{N}_1\text{-M-N}_5$	161.38(6)	$\text{N}_5\text{-M-N}_3$	94.12(7)
$\text{N}_1\text{-M-N}_2$	60.94(5)	$\text{N}_5\text{-M-N}_4$	95.18(7)
$\text{N}_1\text{-M-N}_3$	94.50(6)	$\text{N}_2\text{-M-N}_3$	120.40(6)
$\text{N}_1\text{-M-N}_4$	95.36(6)	$\text{N}_2\text{-M-N}_4$	117.97(6)
$\text{N}_5\text{-M-N}_2$	100.50(6)	$\text{N}_3\text{-M-N}_4$	117.70(7)

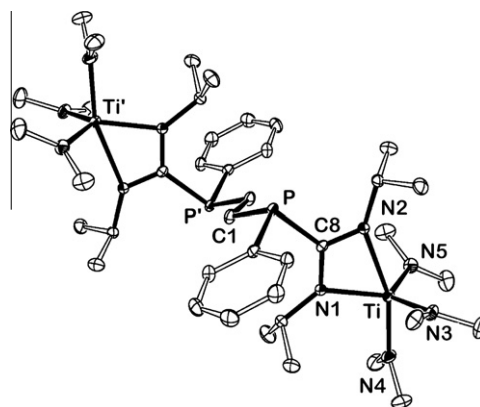


Fig. 8. ORTEP of the molecular structure of  $[\text{PhP}\{C(\text{N}^i\text{Pr})_2\text{Ti}(\text{NMe}_2)_3\}\text{CH}_2-]_2$  (**8a**). Ellipsoids drawn at 30% probability; hydrogens omitted.

In the solid-state the metals adopt a trigonal bipyramidal geometry with the *N,N'*-chelate spanning an axial and equatorial position. Unequal contribution to the bonding from different resonance forms results in localization within the amidine unit, with the greater CN bond-order to the  $\text{N}_{\text{axial}}$  atom. Two conformers are found that differ in the position of the phosphorus substituents, related by rotation about the  $\text{R}_2\text{P-CN}_2$  bond. It is probable that subtle steric effects involving the amide, amidine and phosphorus substituents dictate which of these forms has the lowest energy. This methodology was also extended to the bimetallic complex,  $[\text{PhP}\{C(\text{N}^i\text{Pr})_2\text{Ti}(\text{NMe}_2)_3\}\text{CH}_2-]_2$ , which crystallized as the *meso*-compound, with similar bonding parameters to those observed in the mono-phosphaguanidinate. We are currently examining the suitability of these compounds to act as metal-functionalized ligands in the development of multi-metallic systems for tandem catalysis.

## Acknowledgements

The University of Sussex and the EPSRC are thanked for financial support.

## Appendix A. Supplementary data

CCDC 659262, 659263, 659264, 659265, 659266, 659267 and 659268 contain the supplementary crystallographic data for **3a**, **3b**, **4b**, **5a**, **6a**, **6b** and **8a**. These data can be obtained free of charge via [www.ccdc.cam.ac.uk/conts/retrieving.html](http://www.ccdc.cam.ac.uk/conts/retrieving.html), or from the Cambridge Crystallographic Data Centre, 12 Union Road, Cambridge CB2 1EZ, UK; fax: (+44) 1223-336-033; or e-mail: [deposit@ccdc.cam.ac.uk](mailto:deposit@ccdc.cam.ac.uk). Supplementary data associated with this article can be found, in the online version, at [doi:10.1016/j.poly.2010.05.017](https://doi.org/10.1016/j.poly.2010.05.017).

## References

- [1] D.H.M.W. Thewissen, H.P.M.M. Ambrosius, H.L.M.V. van Gaal, J.J. Steggerda, J. Organomet. Chem. 192 (1980) 101.
- [2] E. Hey-Hawkins, F. Lindenberg, Z. Naturforsch. 48b (1993) 951.
- [3] F. Lindenberg, J. Sieler, E. Hey-Hawkins, Polyhedron 15 (1996) 1459.
- [4] J. Barker, M. Kilner, Coord. Chem. Rev. 133 (1994) 219.
- [5] F.T. Edelman, Coord. Chem. Rev. 137 (1994) 403.
- [6] F.T. Edelman, Top. Curr. Chem. 179 (1996) 113.
- [7] P.J. Bailey, S. Pace, Coord. Chem. Rev. 214 (2001) 91.
- [8] F.T. Edelman, Adv. Organomet. Chem. 57 (2008) 183.
- [9] F.T. Edelman, Chem. Soc. Rev. 38 (2009) 2253.
- [10] M.P. Coles, Chem. Commun. (2009) 3659.
- [11] M.P. Coles, Dalton Trans. (2006) 985.
- [12] J. Grundy, M.P. Coles, P.B. Hitchcock, Dalton Trans. (2003) 2573.
- [13] M.P. Coles, P.B. Hitchcock, Chem. Commun. (2002) 2794.
- [14] G. Jin, C. Jones, P.C. Junk, K.-A. Lippert, R.P. Rose, A. Stasch, New J. Chem. 33 (2009) 64.
- [15] W.-X. Zhang, M. Nishiura, Z. Hou, Chem. Commun. (2006) 3812.
- [16] W.-X. Zhang, Z. Hou, Org. Biomol. Chem. 6 (2008) 1720.
- [17] M.R. Crimmin, A.G.M. Barrett, M.S. Hill, P.B. Hitchcock, P.A. Procopiou, Organometallics 27 (2008) 497.
- [18] T.M.A. Al-Shboul, G. Volland, H. Görls, M. Westerhausen, Z. Anorg. Allg. Chem. 635 (2009) 1568.
- [19] A.J. Roering, S.E. Leshinski, S.M. Chan, T. Shalumova, S.N. MacMillan, J.M. Tanski, R. Waterman, Organometallics 29 (2010) 2557.
- [20] W.-X. Zhang, M. Nishiura, T. Mashiko, Z. Hou, Chem. Eur. J. 14 (2008) 2167.
- [21] N.E. Mansfield, M.P. Coles, P.B. Hitchcock, Dalton Trans. (2005) 2833.
- [22] N.E. Mansfield, M.P. Coles, P.B. Hitchcock, Dalton Trans. (2006) 2052.
- [23] L.S. Baugh, E. Berluce, P.V. Hinkle, F.C. Rix, US Patent US 7351845 B2, 2008.
- [24] N.E. Mansfield, J. Grundy, M.P. Coles, A.G. Avent, P.B. Hitchcock, J. Am. Chem. Soc. 128 (2006) 13879.
- [25] G. Jin, C. Jones, P.C. Junk, A. Stasch, W.D. Woodul, New J. Chem. 32 (2008) 835.
- [26] C. Jones, Coord. Chem. Rev. 254 (2010) 1273.
- [27] J. Grundy, N.E. Mansfield, M.P. Coles, P.B. Hitchcock, Inorg. Chem. 47 (2008) 2258.
- [28] N.E. Mansfield, M.P. Coles, A.G. Avent, P.B. Hitchcock, Organometallics 25 (2006) 2470.
- [29] D.C. Bradley, I.M. Thomas, J. Chem. Soc. (1960) 3857.
- [30] D.G. Dick, R. Rousseau, D.W. Stephan, Can. J. Chem. 69 (1991) 357.
- [31] G.M. Sheldrick, SHELXL-97, Program for the Refinement of Crystal Structures, Göttingen, 1997.
- [32] D. Wood, G.P.A. Yap, D.S. Richeson, Inorg. Chem. 38 (1999) 5788.
- [33] P.J. Bailey, K.J. Grant, L.A. Mitchell, S. Pace, A. Parkin, S. Parsons, J. Chem. Soc., Dalton Trans. (2000) 1887.
- [34] M.P. Coles, P.B. Hitchcock, J. Chem. Soc., Dalton Trans. (2001) 1169.
- [35] A.P. Duncan, S.M. Mullins, J. Arnold, R.G. Bergman, Organometallics 20 (2001) 1808.
- [36] M.P. Coles, P.B. Hitchcock, Organometallics 22 (2003) 5201.
- [37] P. Bazinet, D. Wood, G.P.A. Yap, D.S. Richeson, Inorg. Chem. 42 (2003) 6225.
- [38] X.-A. Pang, Y.-M. Yao, J.-F. Wang, H.-T. Sheng, Y. Zhang, Q. Shen, Chin. J. Chem. 23 (2005) 1193.
- [39] M. Zhou, H. Tong, X. Wei, D. Liu, J. Organomet. Chem. 692 (2007) 5195.
- [40] M. Zhou, S. Zhang, H. Tong, W.-H. Sun, D. Liu, Inorg. Chem. Commun. 10 (2007) 1262.
- [41] S.E. Potts, C.J. Carmalt, C.S. Blackman, F. Abou-Chahine, D. Pugh, H.O. Davies, Organometallics 28 (2009) 1838.
- [42] C.J. Carmalt, A.C. Newport, S.A. O'Neill, I.P. Parkin, A.J.P. White, D.J. Williams, Inorg. Chem. 44 (2005) 615.
- [43] A. Baunemann, D. Rische, A. Milanov, Y. Kim, M. Winter, C. Gemel, R.A. Fischer, Dalton Trans. (2005) 3051.
- [44] A. Baunemann, M. Winter, K. Csapek, C. Gemel, R.A. Fischer, Eur. J. Inorg. Chem. (2006) 4665.
- [45] A. Baunemann, M. Lemberger, A.J. Bauer, H. Parala, R.A. Fischer, Chem. Vap. Dep. 13 (2007) 77.
- [46] D. Rische, H. Parala, A. Baunemann, T. Thiede, R.A. Fischer, Surf. Coat. Technol. 201 (2007) 9125.
- [47] A. Baunemann, D. Bekermann, T.B. Thiede, H. Parala, M. Winter, C. Gemel, R.A. Fischer, Dalton Trans. (2008) 3715.
- [48] C.B. Wilder, L.L. Reifort, K.A. Abboud, L. McElwee-White, Inorg. Chem. 45 (2006) 263.
- [49] D. Rische, A. Baunemann, M. Winter, R.A. Fischer, Inorg. Chem. 45 (2006) 269.
- [50] D. Rische, H. Parala, E. Gemel, M. Winter, R.A. Fischer, Chem. Mater. 18 (2006) 6075.
- [51] A.P. Milanov, T.B. Thiede, A. Devi, R.A. Fischer, J. Am. Chem. Soc. 131 (2009) 17062.
- [52] A.W. Addison, T.N. Rao, J. Chem. Soc., Dalton Trans. (1984) 1349.
- [53] J. Grundy, M.P. Coles, P.B. Hitchcock, New J. Chem. 28 (2004) 1195.
- [54] M.J. McNevin, J.R. Hagadorn, Inorg. Chem. 43 (2004) 8547.
- [55] J.-F. Li, S.-P. Huang, L.-H. Weng, D.-S. Liu, Eur. J. Inorg. Chem. (2003) 810.
- [56] J.-F. Li, S.-P. Huang, L.-H. Weng, D.-S. Liu, J. Organomet. Chem. 691 (2006) 3003.
- [57] G. Häfelinger, K.H. Kuske, The Chemistry of the Amidines and Imidates, Wiley, Chichester, 1991.
- [58] M.P. Coles, D.C. Swenson, R.F. Jordan, V.G. Young Jr., Organometallics 16 (1997) 5183.